International Journal of Scientific Engineering and Technology (ISSN : 2277-1581)
Volume No.2 Issue No.11 pp : 1098 - 1102 1 Nov. 2013

Nucleus-Nucleus (Non-monotonic) Potentials and Vector Analyzing Powers of ^{6}Li Scattering by ^{16}O

Pretam k. Das[1,2] , samiron k. Saha[1]
Department of Physics, Pabna University of Science and Technology, Pabna, Bangladesh .

Email : pretam_nphy@yahoo.com

Abstract:
The data on the elastic scattering cross-section (CS) and vector analyzing power (VAP) of ^{6}Li incident on ^{16}O nuclei is analyzed in terms of an optical model (OM) potential, the real part of which is generated from a realistic two-nucleon interaction using the energy-density functional (EDF) formalism. The EDF-generated real part of the potential is non-monotonic (NM) in nature. This NM real potential part, without any renormalization, along with an emperically determined imaginary part and spin-orbit potential, embodying theunderlying physics of projectile excitation, can successfully account for both CS and VAP data in all cases.

Keywords**: Elastic and quasielastic scattering, Optical and diffraction models, Non-monotonic.**

I. Introduction:

Knowledge of ion-ion potential is a key ingredient to the estimation of cross-sections of elastic scattering and non-elastic processes including the fusion reactions and fragmentation needed for important applications and also to get an answer to a fundamental question of how heavy elements are formed in the universe. The widely used phenomenological potentials of Wood-Saxon (WS) [1] and squared WS (SWS) [2] types suffer from discrete ambiguities, as observed by Mohr et al. [3] in addition to the continuous ambiguities [4]. Standard optical model potentials are usually deep and monotonic. Fits to angular distribution of cross-section with these folding potentials require, in general, an empirical folding renormalization factor that is suggested to be related to unaccounted higher order processes etc. An alternative method for deriving a nucleus-nucleus microscopic potential is the energy-density functional (EDF) theory. In this method , the real part of the potential is the difference in the total energies of the two interacting nuclei at finite and infinite separations. The essential ingredients of the EDF theory for generating successful non-monotonic (NM) potentials are: (i) the Bruckner, Gammel and Thaler [7] two-nucleon (NN) potential including a tensor part, and (ii) explicit consideration of the Pauli principle [9]. This type of potential, with NM characteristics in the real part with $J_R/(4A) \approx 100$ MeV.fm^3 is due to Malik and his co-workers [6]. The NM potential is derivable from a realistic NN potential [9] using the EDF theory [7,8] with full consideration of the Pauli principle. The NM potential is also found consistent in the variations of the volume integral of real with incident energy [5]. The NM α-potential has been also found successful in describing the transfer reactions, where WS and SWS potentials are found inadequate. It would be of interest to see how the nuclear processes induced by medium- and heavy-ion projectiles, can be described by the NM potential with its simple parametrization.The investigation of elastic scattering of ^{7}Li projectiles is considerable interest because this ion with a mass number lies between light ions ($A \leq 4$) and heavy ions ($A \geq 12$) and is expected to exhibit transitional features between the light and heavy ions. Here, ^{6}Li elastic scattering angular distribution data for target ^{16}O are studied at different energies. ^{6}Li have spin and hence potentials of ^{6}Li should include spin-dependent parts along with the central one. While ^{6}Li, with spin $S(^{6}\text{Li})=1$, has both first- and second-rank spin-orbit (SO) terms; bears up to third-rank SO terms in the total potential. Therefore, analyses of the elastic scattering data using polarized ^{6}Li from nuclei are essential for extracting vector and tensor terms of the ^{6}Li-nucleus interactions. In addition, study of polarization phenomena is of general importance to investigate the dynamics of ^{6}Li-nucleus collisions, where the system may be considered as test case to study the effects arising from coupling to breakup channels. The results are also useful to the understanding of nucleus-nucleus collisions using heavy ions as projectile.In this work the *CS* data of the ^{6}Li scattering are studied on ^{16}O target . We analyze the experimental angular distributions of differential cross- sections and vector analyzing powers of ^{6}Li + ^{16}O elastic scattering at different energies in terms of the real part of the NM potential, generated from the EDF calculation, with empirically searched imaginary and effective spin-orbit (SO) potentials in the framework of optical model (OM) calculations and study the energy dependence of the parameters of the imaginary potential.

The analysis is done using the code SFRESCO [30] in the framework of OM. SFRESCO combines the chi-square minimization code MINUIT[25] with the erstwhile coupled-channels code FRESCO [24] .The EDF calculations with a nuclear energy density functional correctly incorporating Pauli effects provide an option to generate nucleus-nucleus potentials from first principles. Therefore, in this work, it was attempted to describe these data using nuclear real potentials obtained from the EDF calculation without any further adjustments of parameters. Only parameters of the imaginary and spin-orbit terms are phenomenologically obtained. It is indeed interesting to observe that without any manipulation of the real nuclear part, it is possible to describe the CS data. It may be noted here that the parameters used in the nuclear energy density functional here lead to a satisfactory description of binding

energies over a wide range of masses for a unique value of the nuclear incompressibility *K* [21]. Furthermore, the position of ^{6}Li in the chain of nucleosynthesis adds extra significance in nuclear astrophysics to the understanding of its interaction potential with other nuclei.

II. Material and Methodology: Energy density functional (EDF) formalism : The shallow non-monotonic molecular (NMM) potential is embedded in the early works of Block and Malik [37, 38], who recognized this potential as a manifestation of the role due to the Pauli exclusion principle and is obtainable from the EDF formalism . In this formalism, the total energy of a system of fermions is described as a functional of the local density, which comprises of a nuclear matter part along with Coulomb corrections as well as corrections for the variable nuclear density (non-homogeneity corrections) in the form of a term involving the gradient of the density.A microscopic approach for obtaining the real part of the nucleus-nucleus potential in the EDF theory employs a realistic *N-N* potential of Brueckner, Gammel, and Thaler (BGT). The BGT potential describes all the properties of deuteron and observed phase-shifts up to about pion-production energy. Moreover, in the EDF theory the Pauli principle is considered in determining the mean-field in nuclear and nucleonic matter approximation. The starting point of the EDF theory is the theorem that the energy of a system of fermions for a given density distribution $\rho(r)$ can be expressed as $E = \int \varepsilon\left[\rho(\vec{r})\right] d^3\vec{r},$ (1)

where $\varepsilon\left[\rho(\vec{r})\right]$, the energy density, is given by

$$\varepsilon\left[\rho(\vec{r})\right] = 0.3\left(\frac{\hbar^2}{2M}\right)\left(\frac{3\pi^2}{2}\right)^{2/3}\left[(1-\xi)^{5/3}+(1+\xi)^{5/3}\right]\rho^{5/3} + \nu(\rho,\xi)\rho + \frac{e}{2}\Phi_C(\vec{r})\rho_P - 0.739\,e^2{\rho_P}^{4/3} + \left(\frac{\hbar^2}{8M}\right)\eta\left(\vec{\nabla}\rho\right)^2. \quad (2)$$

Here, *M* is the nucleon mass and $\xi = (N-Z)/A$ is the neutron excess parameter. The first term in (2) arises from the nucleon kinetic energy in nuclear matter. The nucleonic mean field $\nu(\rho,\xi)$ is determined from the BGT *N-N* potential [07] in Brueckner-Hartree-Fock approximation theory [09] of nuclear matter. This theory relates the matrix elements of the potential [09] to those of scattering operator *K* with full consideration of the Pauli principle among the nucleons of the same type in the nuclear and nucleonic matter approximation, *i.e.*, using plane wave for nucleonic wave functions. The density dependence of energy per nucleon E/A in this nuclear matter has been calculated by Brueckner *et al*. [09] using this potential with consideration of Pauli principle. The calculated $\nu(\rho,\xi)$ has been parametrized analytically as

$$\nu(\rho,\xi) = b_1\left(1+a_1\xi^2\right)\rho + b_2\left(1+a_2\xi^2\right)\rho^{4/3} + b_3\left(1+a_3\xi^2\right)\rho^{5/3}. \quad (3)$$

The coefficients, a_1 = -0.200, a_2 = 0.316 and a_3 = 1.646, b_1 = -741.28, b_2 = 1179.89, and b_3 =-467.54, are derived [39] from fitting the calculated curves for the density distribution of the energy per nucleon, E/A. Hence the nucleon potential in the mean field incorporates the exchange effects. The Coulomb energy Φ_C in (2) is related to the proton charge density distribution ρ_P as

$$\Phi_C = e\int \frac{\rho_P(\vec{r}')}{|\vec{r}-\vec{r}'|}\, d^3\vec{r}'. \quad (4)$$

The fourth term represents the exchange correction among the protons due to the Coulomb energy. The fifth term is the inhomogeneity correction, which incorporates the correction part of the nuclear interaction not included in the mean field. This term includes a parameter η [39]. An optimum value of $\eta = 8.0$ has been found to reproduce the observed nuclear masses [39] and hence, binding energies, of the nuclei in the range from ^{12}C to ^{238}U to within 1.5%.

The potential $V(R)$ between the projectile P and the target T at a separation distance of R is given by

$$V(R) = E\left[\rho(\vec{r},R)\right] - E_P\left[\rho_P(\vec{r},R=\infty)\right] - E_T\left[\rho_T(\vec{r},R=\infty)\right], \quad (5)$$

where ρ is the density distribution function (DDF) of the composite system. Here, ρ_P and ρ_T are, respectively, the DDFs for the projectile and the target at $R=\infty$. In the sudden approximation, the DDF of the composite system is given by

$$\rho(r) = \rho_P(r) + \rho_T(r). \quad (6)$$

Non-monotonic molecular (NMM) potential: Energy-density functional (EDF) formalism calculations in the sudden approximation [22], in general, leads to a shallow non-monotonic molecular (NMM) type real part of nucleus-nucleus potential. The NMM potential, at a given projectile energy, has the following form [23] for the real, $V_{NMM}(R)$ and imaginary, $W_{NMM}(R)$ parts:

$$V_{NMM}(R) = -V_0\left[1+\exp\left(\frac{R-R_0}{a_0}\right)\right]^{-1} + V_1\exp\left[-\left(\frac{R-D_1}{R_1}\right)^2\right] + V_C(R), \quad (7)$$

$$W_{NMM}(R) = -W_0\exp\left[-\left(\frac{R}{R_W}\right)^2\right] - W_S\exp\left[-\left(\frac{R-D_S}{R_S}\right)^2\right] \quad (8)$$

In Eq. (7), V_1 and R_1 are respectively the depth and radius of repulsive core. The real part of the molecular potential is non-monotonic due to the presence of second term in (8), which results in a short-range repulsive core. The Coulomb radius R_C, in the NMM potential is the sum of the radii of the charge density distributions of projectile and the target nucleus, as explained in [23]. The imaginary part in (7) includes both the volume term with the Gaussian shape and a surface absorption term with the shifted Gaussian one.

Generation of nuclear potentials from EDF: The real nuclear part of the central potentials for ^{6}Li are obtained from the Energy Density Functional (EDF) theory. Details for the EDF calculations can be found in [22]. This

involves two sets of input: (a) the nuclear energy density functional and (b) the density distribution (DD) functions for the interacting nuclei.

The parameter values [5] for the nucleonic mean potential with full consideration of the Pauli principle are $a_1 = -0.2$, $a_2 = 0.316$ and $a_3 = 1.646$, $b_1 = -741.28$, $b_2 = 1179.89$ and $b_3 = -467.54$, which correspond to K =187.0 MeV [20], ε =-16.59 and Fermi momentum k_F=1.447 fm^{-1} at saturation density,ρ_0=0.202. The density distribution parameters used are given in Table 1. The choice is made considering the quality of reproduction of the binding energies.

The EDF calculations also involves the sudden approximation $\rho(r) = \rho_P(r) + \rho_T(r)$ with *P* and *T* referring to the projectile and target, respectively. The sources of the DD functions are [34] for ^{6}Li;and [32] for ^{16}O. These DD functions are transformed to the two-parameter Fermi (2pF) function, $\rho(r) = \rho_0[1+\exp((r-c)/z)]^{-1}$ for use in the EDF calculations. The deduced parameters are given in Table 1.

The EDF-calculations then provide the shape of the real part of the nuclear potential. This is observed to have a non-monotonic (NM) form with a central part that becomes repulsive. The derived real parts of the ^{6}Li NM potentials are shown in solid dots in Figs. 1. These potentials are then parametrized in terms of the simple analytic expression:

$$V(R) = -V_0\left[1+\exp\left(\frac{R-R_0}{a_0}\right)\right]^{-1} + V_1\exp\left[-\left(\frac{R}{R_1}\right)^2\right] \quad (9)$$

and the parametrized potential is shown in solid lines. The second gaussian term is added to the usual Woods-Saxon or Fermi term to account for the repulsive core.

Table 1: The parameters of the equivalent 2pF density distribution (DD) function for the nuclei with the sources given in the text, c and z are in fm, ρ_0, in fm^{-3} and the binding energy, in MeV.

Nucleus	Parameters of 2pF density function			Binding energy	
	c	z	ρ_0	Calculation	Experiment
^{6}Li	1.333	0.561	0.2118	33.2	32.0
^{16}O	2.525	0.450	0.181	129.5	127.6

The Coulomb potential V_C of a uniformly charged sphere with radius R_C is added to obtain the total real part of the potential. The real nuclear parameters, derived in the above-mentioned way from the EDF-generated ^{6}Li potentials, are given in Table 2 along with the volume integrals $J_R/(A_P A_T)$ and R_C.**Table 2:** Analytic parameters in of the EDF-generated NM projectile-target (system) potential along with the Coulomb radius R_C and the volume integral $J_R/(A_P A_T)$. The incident energy (E_{Li}) and depth parameters are in MeV, the geometry parameters are in fm and in MeV.fm^{-3}.

System	V_0	R_0	a_0	V_1	R_1	R_C	$J_R/(A_P A_T)$
^{6}Li+^{16}O	48.37	4.38	0.779	42.60	3.5	7.68	126.7

Spin-orbit and imaginary parts of the potential: The imaginary part of the ^{6}Li-potential is taken phenomenologically to be composed of volume and surface terms as

$$W(R) = -W_0\exp\left[-\left(\frac{R}{R_W}\right)^2\right] - W_S\exp\left[-\left(\frac{R-D_S}{R_S}\right)^2\right]. \quad (10)$$

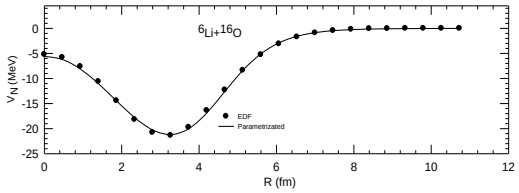

Fig. 1 Parametrization of the solid lines with the analytic expression given in fitting the nuclear part $V_N(R)$ of the EDF-generated ^{6}Li-^{16}O potentials (solid dot) using DD functions given in Table 1. The generated potential parameters are noted in Table 2 .

The effective SO part of ^{6}Li potentials is assumed to have the standard WS form with only the real part as

$$U_{SO}(R) = 2\frac{V_{SO}}{R}\frac{d}{dR}\left[1+\exp\left((R-R_{SO})/a_{SO}\right)\right]^{-1}\vec{l}.\vec{I} \quad (11)$$

Here, *l* and *I* are, respectively, the partial wave and spin of ^{6}Li. The depth parameter V_{SO}, and the geometry parameters R_{SO} and a_{SO} have been adjusted for the best possible fit to the vector analyzing power (VAP) data.

III. Results and Tables: Optical Model analyses have been carried out using the code SFRESCO, which incorporates the coupled-channels code FRESCO 2.5 [24] coupled with the χ^2-minimization code MINUIT [25].The experimental cross-section (CS) and iT_{11} data have been taken from [34] for ^{6}Li-^{16}O at 22.8 MeV and for ^{6}Li-^{16}O at 25.7 MeV. The experimental cross-section (CS) data has been taken from [27] for ^{6}Li-^{16}O at 4.5 MeV, 20 MeV and 50.6 MeV. The experimental cross-section data has been taken from [36] for ^{6}Li-^{16}O at 48 MeV. The experimental cross-section data has been taken from [32] for ^{6}Li-^{16}O at 13 MeV, 29.8 MeV and 36 MeV. The experimental cross-section data has been taken from [35] fot ^{6}Li-^{16}O at 50 MeV.A systematic error of 15% has been assumed for the experimental *CS* data normalized to

the Rutherford cross-sections (σ/σ_R) for the angular points without the error bars. In simultaneous analysis of the *CS*, the EDF-generated parameters for the real part of the ^{6}Li-target potentials, given in Table 2 have been held fixed. The fits to the *CS* has been optimized in first by minimizing the χ^2. Final fits have been done visually after taking guidance from the χ^2 fits, since it is more important to reproduce the features e.g. positions of the peaks etc., of the angular distributions than naively minimizing the χ^2 only. The final parameters for the imaginary and SO potentials are noted in Tables 3 , 4. One can see that the effective SO strength are either attractive with positive sign of the depth V_{SO} or repulsive with the negative depth..

Table 3: Empirical imaginary and SO parameters of the projectile-target (system) potential along with the total χ^2 per point on combined fits to *CS* data . The incident energy (E_{Li}) and depth parameters are in MeV, and the geometry parameters, in fm.

E	W_S	d_S	R_S	W_0	R_W	V_{so}	r_{so}	a_{so}	$J_I/6A$	χ^2
4.5	5	1.4	0.11	3.0	4.4	0.6	1.7	0.5	16.3	0.340
13.0	71	1.4	0.11	3.5	4.4	0.6	1.7	0.5	40.1	22.29
20.0	41	1.4	0.11	9.0	4.4	0.6	1.7	0.5	57.3	14.09
22.8	35	1.4	0.11	11.0	4.4	0.3	1.7	0.5	65.2	13.97
25.7	23	1.4	0.11	12.0	4.4	0.2	1.7	0.5	66.0	16.83
48.0	2.6	1.4	0.11	20.5	4.4	0.6	1.7	0.5	101.2	44.43
50.6	1	1.4	0.11	23.5	4.4	0.6	1.7	0.5	115.3	16.03

Fig.3 The OM predicted σ/σ_R (solid lines) for the ^{6}Li elastic scattering on ^{16}O using the parameters of the EDF-generated real central potential (table 2) , and the empirical imaginary and effective SO potentials (table 3), are compared with the experimental data.

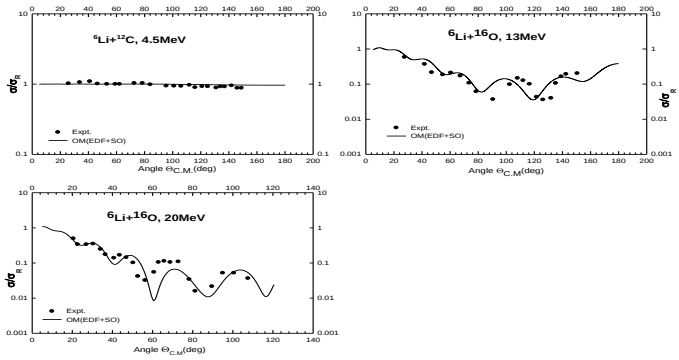

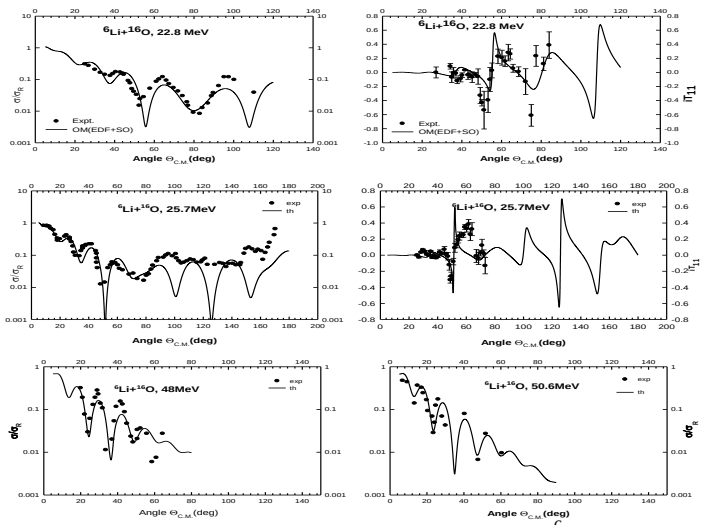

Fig.3 The OM predicted σ/σ_R (solid lines) for the ^{6}Li elastic scattering on ^{16}O using the parameters of the EDF-generated real central potential (table 2) , and the empirical imaginary and effective SO potentials (table 3), are compared with the experimental data.

Figure 3 presents the comparison between the cross-sections predicted by the EDF generated potentials and the experimental data of ^{6}Li elastic scattering on ^{16}O predicted by the EDF generated potentials, and corresponding experimental data. The parameters of the EDF generated potential describe the data well, including the wide angular distributions, without any need for adjustment of parameters or renormalization of the potential up to the 13MeV. The EDF generated potential parameters displayed in Table 2 along with those for the imaginary part, the volume integrals, $J_I/(6A)$, and the χ^2 values for the fits are displayed in Table 3. Here it is observed that the surface parameters d_S and R_S and geometry parameters R_w are fixed while W_S and W_0 are changed with energy. It is attempted to keep the value of the χ^2 minimum. The imaginary potential in Table 3 can reproduced both CS data well without changing the real part

IV. Conclusion: The EDF theory, as used in the present study, reproduces the correct binding energies of the projectile ^{6}Li and ^{16}O target remarkably well using the available density distributions with the appropriate RMS radii. Hence, considering the consistencies in the volume integrals and observed their variations with respect to incident energies in [5] and in Table 2 of the present work, the performance of the NM potential generated from EDF is well in describing the elastic scattering of ^{6}Li. The *CS* data are reproduced well simultaneously with the unadjusted real parameters generated from the EDF calculations with the exception for the *CS* data for ^{16}O. The latter, as shown explicitly in the work of Basak et al. [21], is generated from the projectile excitation processes and the imaginary potential provided the real part of the ^{6}Li potential has the appropriate NM nature. The NM nature of the real part of the

central ^{6}Li potentials, as indicated in [19,21], also plays a significant role, along with the dynamics of the projectile excitation, in producing the dynamic polarization potential (DPP) effects responsible for producing the effective spin orbit (SO) potential. The fact that the EDF-generated NM potential does not need any normalization is ensured by: (i) the appropriate use of the Pauli principle and (ii) the validity of sudden approximation for the composite system of the projectile and target nuclei.WS potential is monotonic and it goes into saturation after becoming maximum. On the other hand, our non-monotonic (NM) molecular potential does not go into saturation. There is a repulsive term is included due to Pauli principle.Very recently, Basak et al., [21] has shown that the NM feature of the real central potential in conjunction with appropriate imaginary potentials can produce correct SO potentials to describe the VAP data of ^{6}Li elastic scattering. In conclusion, the NM nature of real part of the central ^{6}Li-nucleus potential, along with the dynamics of the projectile excitation, seems to play a significant role in producing the proper DPP responsible for generating the actual effective SO potential to reproduce the CS an all cases and of ^{6}Li elastic scattering.

Acknowledgement:I am indebted to Prof.Emeritus Dr. Arun Kumar Basask, and Dr. Abdullah shams bin tariq, Nuclear Physics Lab,University of Rajshahi for helping me in this research and also thankfully acknowledged.

References:

i. *A.T. Rudchik et al., Phys. Rev. C 75 (2007) 024612.*
ii. *M.F. Vineyard et al., Nucl. Phys. A 405(1983) 429.*
iii. *P. Mohr et al., Phys. Rev. C 55 (1997) 1523.*
iv. *G.R. Satchler, Direct Nuclear Reactions, Clarendron Press, Oxford, 1983.*
v. *S. Hossain et al., Eur.Phys. J. A 41 (2009) 215*
vi. *P. Manngard et al., Eur.Phys. J. A 41 (2009) 215*
vii. *K.A. Brueckner, J.L.Gammel, Phys. Rev. 109 (1989) 1023*
viii. *K.A. Brueckner, J.R. Bucher, M.M. Kelly, Phys. Rev. C 173 (1968) 944*
ix. *K.A. Brueckner, S.A. Coon, J. Dabrowski, Phys. Rev. 168 (1968) 1184.*
x. *M. Liu, N. Wong, Z. Li, X. Wu and E. Zhao, Nucl. Phys. A 768 (2006) 80.*
xi. *A. Devrowski, K. Pomorski and J. Barleb, Nucl. Phys. A 729 (2003) 713.*
xii. *Yu. V. Devison and W. Nörenberg, Eur. Phys. J. A 15 (2002) 388.*
xiii. *A.S.B. Tariq, A.F.M.M. Rahman, S.K. Das, A.S. Mondal, M.A. Uddin, A.K. Basak, H.M. Sen Gupta, F.B. Malik, Phys. Rev. C 59 (1999) 2558.*
xiv. *S.K. Das, A.S.B. Tariq, M.A. Uddin, A.S. Mondal, A.K. Basak, K.M. Rashid, H.M. Sen Gupta, F.B. Malik, Phys. Rev. C 62 (2000) 054606.*
xv. *M.N.A. Abdullah, M.S. Mahbub, S.K. Das, A.S.B. Tariq, M.A. Uddin, A.K. Basak, H.M. Sen Gupta, F.B. Malik, Eur. Phys. J. A 15 (2002) 477.*
xvi. *]S. Hossain, M.N.A. Abdullah, S.K. Das, M.A. Uddin, A.K. Basak, H.M. Sen Gupta, I J. Thompson and F.B. Malik et al., J. Phys. G 31 (2005) 309.*
xvii. *M.N.A. Abdullah, A.B. Idris, A.S.B. Tariq, M.S. Islam, S.K. Das, M.A. Uddin, A.S. Mondal, A.K. Basak, I. Reichstein, H.M. Sen Gupta, F.B. Malik, Nucl. Phys. A 760 (2005) 40.*
xviii. *M.M. Billah, M.N.A. Abdullah, S.K. Das, M.A. Uddin, A.K. Basak, I. Reichstein, H.M. Sen Gupta, F.B. Malik, Nucl. Phys. A 762 (2005) 50.*
xix. *S. Hossain, M.N.A. Abdullah, A.S.B. Tariq, M. A. Uddin, A. K. Basak, K.M. Rusek , I. Reichstein and F. B. Malik, Europhys. Lett. 84 (2008) 52001.*
xx. *Pozdnyakov, A.V. Reichstein I., Shehadeh Z.F. and Malik F.B., condensed matter theories 10(1995) 365.*
xxi. *A.K. Basak, M.M. Billah, M.J. Kobra, M.K. Sarkar, M. Mizanur Rahman, Pretam K. Das, S.Hossain, M.N.A. Abdullah, A.S.B. Tariq, M.A. Uddin, S. Bhattacharjee, I. Reichestein and F.B. Malik EPL, 94 (2011) 62002 .*
xxii. *F. B. Malik and I. Reichstin, Clustering Phenomena in Atoms and Nuclei, eds M. Brenner, T. Lönnroth and F.B. Malik (Springer-Verlag, Berlin, Heidelberg,1992), p.126.*
xxiii. *M.M. Billah, M.N.A. Abdullah, S.K. Das , M.A. Uddin , A.K. Basak, I. Reichstein, H.M. Sen Gupta, F.B. Malik, Nucl. Phys. A 762 (2005) 50.*
xxiv. *I.J. Thompson, Comp. Phys. Rep. 7 (1988) 167.*
xxv. *F. James, M. Roos, Comput. Phys. Commun. 10 (1975) 343.*
xxvi. *K.H. Bray, Mahavir Jain, K.S. Jayaraman, G. Lobianco, G.A. Moss, W.T.H. van Oers, D.O. Wells, F. Petrovich, Nucl. Phys. A 189 (1972) 35.*
xxvii. *M.F. Vineyard, J. Cook, K.W. Kemper Phys. Rev. C 30 (1984) 916*
xxviii. *F. Michel, S. Ohkubo, Phys. Rev. C 72 (2005) 054601*
xxix. *Y. Hirabayashi, Phy. Rev. C 44 (1991) 1581.*
xxx. *I.J. Thompson, Sfresco, version 2.5 University of surrey, Guildford GU2 7XH, England and Livermore National laboratory, Livermore CA 94551, USA, 2008.*
xxxi. *Basak A.K. et. al., Phys lett. B, 692 (2010) 47*
xxxii. *A.K. Chaodhuri and Bikash Sinha, Nuclear Phys. A455(1986)169-178.*
xxxiii. *M.F. Vineyard, J. Cook, K.W. Kemper, and M.N. Stephens, Phys. Rev. **30** (1984) 3.*
xxxiv. *S.P. Van verst, D.E. Trcka, K.W. Kemper Phys. Rev. C 39 (1989) 853.*
xxxv. *D.E. Trcka, A.D. Frawley et. al., Phys. Rev. C41 (1990) 2134*
xxxvi. *J. Cook, L.C. Dennis et. al., Nuclear Phys. Rev. A415 (1984) 114*
xxxvii. *B. Block, F.B. Malik, Phys. Rev. Lett. 19 (1967) 239.*
xxxviii. *L. Rickertsen, B. Block, J.W. Clark, F.B. Malik, Phys. Rev. Lett. 22 (1969) 951.*
xxxix. *M.A. Hooshyar, I. Reichstein, F.B. Malik, Nuclear Fission and*
xl. *Cluster Radioactivity, Springer-Verlag, Berlin, 2005.*